

Preliminary exploration of radiomic mammographic analysis in triple negative breast cancer related to BRCA profile

Received: 16 September 2025

Accepted: 8 January 2026

Published online: 13 February 2026

Cite this article as: Pecchi A., Sessa G., Nocetti L. *et al.* Preliminary exploration of radiomic mammographic analysis in triple negative breast cancer related to BRCA profile. *Sci Rep* (2026). <https://doi.org/10.1038/s41598-026-35774-1>

Annarita Pecchi, Giulia Sessa, Luca Nocetti, Cecilia Beretta, Chiara Bozzola, Erica Balboni, Giulia Besutti, Angela Toss, Laura Cortesi, Gabriele Guidi, Massimo Dominici & Pietro Torricelli

We are providing an unedited version of this manuscript to give early access to its findings. Before final publication, the manuscript will undergo further editing. Please note there may be errors present which affect the content, and all legal disclaimers apply.

If this paper is publishing under a Transparent Peer Review model then Peer Review reports will publish with the final article.

PRELIMINARY EXPLORATION OF RADIOMIC MAMMOGRAPHIC ANALYSIS IN TRIPLE NEGATIVE BREAST CANCER RELATED TO BRCA PROFILE

Authors:

Annarita Pecchi*¹, Giulia Sessa¹, Luca Nocetti², Cecilia Beretta¹, Chiara Bozzola¹, Erica Balboni², Giulia Besutti^{1 4}, Angela Toss³, Laura Cortesi³, Gabriele Guidi², Massimo Dominici³, Pietro Torricelli¹.

*Corresponding author:

Annarita Pecchi

Annarita.pecchi@unimore.it

+39 3397525712

+39 0594225885

¹Division of Radiology, Department of Medical and Surgical Sciences of Children and Adults, University of Modena and Reggio Emilia, 41224 Modena, Italy.

²Medical Physics Unit, University Hospital of Modena, 41124 Modena, Italy.

³Division of Oncology, Department of Medical and Surgical Sciences of Children and Adults, University of Modena and Reggio Emilia, 41224 Modena, Italy.

⁴Radiology Unit, Azienda USL-IRCSS di Reggio Emilia, 42123 Reggio Emilia, Italy.

ABSTRACT

This retrospective study evaluated the applicability of radiomics analysis to mammographic images of patients with triple-negative breast cancer (TNBC) to identify features differentiating BRCA gene's mutational status. The mammographic images of 52 patients histologically diagnosed with TNBC, (13 BRCA-mutated patients and 39 BRCA wild-type ones), were included and 53 tumor lesions were manually segmented in the mammographic projection where they were better demarcable. An additional elliptical ROI of standard size was drawn in the most homogeneous area of the contralateral healthy gland, using the analogue mammographic projection of the same date or, if not available, of the corresponding bilateral mammographic investigation closer to the time of diagnosis. Lesions consisted of 36 masses, 2 pathological microcalcifications, and 15 masses with microcalcifications.

Radiomic features were extracted using Pyradiomics-3D. Preliminary analysis confirmed feasibility and showed differences in texture features, particularly GLCM SumEntropy, between BRCA-mutated and non-mutated patients. Moreover, the study enhanced the role of healthy glandular tissue in distinguishing the two groups, supporting and reinforcing previous MRI-based radiomics findings in the same population. The study concludes that radiomics analysis of diagnostic mammograms in TNBC patients is feasible and may help build predictive models to discriminate between BRCA mutated and non-mutated patients.

KEYWORDS

Radiogenomics

Mammography

Breast cancer

BRCA1 gene

GLCM Sum Entropy

GLOSSARY

- ACR = American College of Radiology
- AUC = Area Under ROC Curve
- BI-RADS = Breast Imaging Reporting & Data System
- BRCA = a gene related to a higher risk of breast cancer
- CLEAR checklist = CheckList for EvaluAtion of Radiomics research
- DCIS = Ductal Carcinoma In Situ
- ER = estrogen receptors
- ESR = European Society of Radiology
- EuSoMII = European Society of Medical Imaging Informatics
- GLCM = gray level co-occurrence matrix
- GLDM=Gray Level Dependence Matrix
- GLRLM=Gray Level Run Length Matrix
- GLSZM= gray level size zone matrix
- Heat-plot maps/ Heat maps = an image that depicts the values of some variables of interest across two axes as a color-coded matrix
- HER-2 = Human Epidermal growth factor Receptor 2
- LCC = Left Craniocaudal
- LML = Left Mediolateral
- LMLO = Left Mediolateral Oblique
- MRI = Magnetic Resonance Imaging
- NGTDM= neighborhood gray-tone difference matrix
- PG =progesterone receptors

- Pyradiomics library= an open-source python package for the extraction of Radiomics features from Medical Imaging
- Python = A programming language that allow to work quickly and integrate systems more effectively.
- RRC = Right Craniocaudal
- RML = Right Mediolateral
- RMLO = Right Mediolateral Oblique
- ROC Curve= Receiver Operating Characteristic curve which is a graphical plot that illustrates the performance of a binary classifier model
- ROI = region of interest
- TNBC= triple negative breast cancer

ARTICLE IN PRESS

1.0 INTRODUCTION

Triple-negative breast cancer (TNBC), accounting for 15–25% of all breast cancers, is a specific subtype of breast cancer that does not express estrogen receptor (ER), progesterone receptor (PR) or human epidermal growth factor receptor 2 (HER-2) [1]. It has clinical features that include high invasiveness, high metastatic potential, proneness to relapse and poor prognosis [2], [3]

TNBC lacks effective targeted therapies such as endocrine therapies and anti-HER2 antibodies, such as trastuzumab.

BRCA1 and BRCA2 are tumor suppressor genes, the mutant phenotypes of which predisposes patients to breast and ovarian cancers [4], [5]

Women with BRCA 1 and BRCA 2 gene mutations have an increased risk of developing breast cancer: by the age of 70 years, the risk is about 56–83%. TNBC has a close association with mutations in the BRCA pathway. Among newly diagnosed breast cancer patients, fewer than 10% have a mutation in the BRCA1 or BRCA2 genes, while more than 16% of TNBC patients are identified with BRCA mutations [5]

Several studies have evaluated the relationships between the BRCA mutation types, mammographic findings and pathologic features of breast cancers [6], as well as the mammographic aspects of TNBC [5].

These studies suggest that mammographic features of tumoral lesions can differ according to BRCA mutation type [4], [5], [6] and that the typical mammographic finding among TNBC patients is a mass with no calcifications, obscured margins and irregular shape [5].

While breast cancer in BRCA1 carriers is more likely to present as TNBC with more aggressive behavior [7] and a more difficult detection on mammography due to benign appearance, which may in part be an effect of rapid growth

rate [8], BRCA2-related tumors are much more similar to sporadic cancer [9], [10]. BRCA2 carriers are more likely to present with ductal carcinoma in situ (DCIS), which more often develops microcalcifications [8].

Radiomics by the side, which is the process of extracting quantitative properties, named features, from an entire image or from a specific region of interest (ROI) collectively providing a comprehensive tumor characterization [11], [12],[13], is emerging as a reliable, accurate, non-invasive, and cost-effective approach to classify breast cancer characteristics and predict patient outcomes by revealing alterations in the tumor histological anatomy that are difficult to quantitatively identify by the human eye [12], [14].

Radiomics in breast cancers is a new emerging field of research. While most of the studies so far provided correlation with histological outcomes and staging variables or biomarkers [15] [16], only a few of them have investigated the correlation between radiomic features and genomic profile, that is radiogenomics, which is gaining importance for tumors characterization [17], [18], [19], [20].

In the specific field of TNBC then, the studies carried out were mainly aimed at identifying radiomic features to distinguish TNBC from other breast lesions and to detect different subtypes of TNBC. Other studies investigated the correlation between radiomic features and biomarkers in order to guide clinical decisions, to evaluate the treatment efficacy and to create predictive and prognostic models [21].

Although most of the studies involved MRI, only a few of radiomics studies have assessed the potential usefulness of mammography-based radiomics to predict breast cancer characteristics such as the molecular subtypes. They even assessed the added value of radiomics, when combined with

clinical data, in predicting factors such as histological grade and invasiveness [14], [22]

In this setting the aim of our study is to evaluate the applicability of radiomics analysis to mammographic images of patients diagnosed with TNBC to identify radiomics features that can differentiate the mutational status of BRCA genes.

2.0 MATERIALS E METHODS

2.1 Study design

We used the CLEAR checklist (CheckList for Evaluation of Radiomics research) endorsed by ESR and EuSoMI to design and report this manuscript [23].

The research was approved by the Area Vasta Emilia Nord Ethical Committee (463/2020/OSS/AOUMO) and informed consent was obtained from all subjects. All methods were performed in accordance with the Declaration of Helsinki. This retrospective study included consecutive patients histologically diagnosed with TNBC and evaluated at the Oncology Department of Modena University Hospital who underwent digital breast mammography between February 2010 and August 2021.

The criteria for patients' inclusion were the histological diagnosis of triple negative ductal invasive breast cancer, the genetic testing result and the availability of a digital mammography at the time of the diagnosis before any medical or surgical treatment. On the other hand, we excluded patients with unavailability of clinical and pathological data, as well as the unavailability of a mammographic examination at the time of the diagnosis.

2.2 Clinical and radiological data collection

Clinical data (age and mutational profile) and imaging data (breast density, number and type of lesions, extension of the disease) were collected with the collaboration of Oncology Department and analyzed with the Medical Physics Unit.

All mammographic exams were performed with digital technique in the standard projections Left Craniocaudal (LLC), Left Mediolateral Oblique (LMLO), Right Craniocaudal (RRC), Right Mediolateral Oblique (RMLO) and/or with additional projections Left Mediolateral (LML) and Right Mediolateral (RML).

Collected non-radiomics data were:

- Patients' age
- Breast density evaluated through subjective analysis in accordance with the recommendations of the proposed American College of Radiology Breast Imaging Reporting and Data System (ACR BI-RADS) and classified in A (almost entirely fatty), B (scattered areas of fibroglandular density), C (heterogeneously dense breasts) and D (extremely dense breast) [24].
- the extent of disease, classified in single lesion or multiple lesions.
- the type of mammographic lesion, classified in accordance with the recommendations of the proposed American College of Radiology Breast Imaging Reporting and Data System (ACR BI-RADS) [24] into mass (nodule), mass with microcalcifications, isolated microcalcifications and distortions.

2.3 Radiomic analysis

Mammographic images were reviewed to collect radiomic data from the tumor and the contralateral gland, which were manually segmented by two radiologists in consensus.

Radiomic data were compared between tumors and contralateral glands of BRCA-mutated and non-BRCA mutated women and different radiomic classifier were tested to predict mutational status.

2.3.1. Segmentation

For each patient the tumor lesion (or lesions, where more than one had been detected) was individuated and manually segmented through a contouring tool including all the visible lesion in Advantage Workstation 4.7 (GE Healthcare) using the mammographic projection where it was better demarkable. The two radiologists together evaluated every single image and decided in consensus on which mammographic projection to segment the lesion. An elliptical Region of Interest (ROI) of standard size (100 mm²) was drawn in the most homogeneous area of the contralateral healthy gland using the analogue mammographic projection of the same date or, if not available, of the corresponding bilateral mammographic investigation closer to the time of diagnosis. (Figure 1-4). The two radiologists in consensus decided the placement of the ROI within the healthy glandular tissue following homogeneity criteria.

We used 17 LCC, 11 LMLO, 8 RCC, 11 RMLO, 3 LML and 2 RML projections for the segmentation of the tumoral lesions, and 8 LCC, 13 LMLO, 17 RCC, and 14 RMLO projections for the segmentation of the healthy glands.

We evaluated inter-rater reliability using the Intraclass Correlation Coefficient (ICC) on a subset of 20 lesion volumes, estimated with a two-way random-effects model assessing absolute agreement.

2.3.2 Preprocessing

Images were normalized by scaling data to a range 0-1 based on the 1st and the 99th percentile with a custom Python routine.

2.3.2. Features extraction

Radiomic features were extracted from the ROIs (described in the Segmentation section) with a custom Python routine through the Pyradiomics library, using a bin number equal to 20 and a symmetrical Gray Level co-occurrence matrix. The other extraction parameters were left as default.

All available features were extracted except for shape features for glandular ROIs since the considered ROIs had a fixed shape.

2.3.4. Features selection and data preparation

The processing of the extracted features and the statistical analyses were performed through a Stata 17 code with Python 3.8 integration, using the Python libraries SK-learn v. 1.0.2, and Numpy v. 1.24.4. The extracted features were standardized by subtracting the mean value and dividing by the standard deviation. We first considered separately the features from the tumor and the contralateral gland, then we performed another analysis with all the features together building three different models: a model with gland features only, a model with tumor features only and a comprehensive model with both tumor and gland features.

For dimensionality reduction, the most important and discriminative features for BRCA status classification were selected with Maximum Relevance Minimum Redundancy algorithm. To decide the number of selected features we visually inspected the correlation heat-plot of all

the features, showing the Spearman correlation matrix in color scale, with rows and columns sorted by similarity via hierarchical clustering (figure 5-7). The number of features corresponded to the number of components derived from Principal Component Analysis (PCA), accounting for 80% of the total variance in the Spearman correlation matrix [25]. Feature standardization and feature selection via mRMR were performed on the complete dataset. While this approach may introduce some data leakage, it allows for a consistent set of selected features and simplifies the application of the final model.

2.3.5. Modelling

The selected features in each model were used to train 4 classifiers, one linear, Logistic Regression, and the other ones non-linear, which were Support Vector Classifier (SVC), Random Forest and Decision Tree. The setting parameters were left as default, i.e. SVC with 1 as regularization parameter; Random Forest with 100 estimators and no maximum depth, as well as for Decision Tree.

2.3.6. Evaluation

The models were internally tested through stratified 10-fold cross validation by permuting 10 times the training (90% of the entire sample) and the testing dataset (10%). Furthermore, the stratified cross validation allowed to keep the same percentage of patients with and without the mutation in each permutation, balancing the two groups. For each model and permutation, we calculated the Area Under ROC Curve (AUC), the accuracy, the sensitivity, and the specificity. The sensitivity and specificity were computed at their optimal value in the ROC curve, maximizing their geometric mean.

Then, we considered the mean and the standard deviation (SD) of these scores across the 10 permutations. As suggested in other studies we used AUC as the discriminant metric to identify the best model [26].

To evaluate if the different models and the classifiers had significant differences, we used the Delong's test.

3.0 RESULTS

3.1 Baseline demographic and clinical characteristics

Among patients with TNBC histological diagnosis from February 2010 to August 2021, we retrospectively selected 52 patients (mean overall age $47,97 \pm 9,4$, mean age of mutated patients $44,99 \pm 10,4$, mean age of non-mutated patients $47,97 \pm 9,4$) who had histological diagnosis of TNBC and performed a mammographic examination at the time of the diagnosis. 13 of the 52 patients were BRCA mutated and 39 were non-BRCA mutated. The mammographic lesions were identified as masses in 36 cases as one patient had two lesions in the same gland, as masses with microcalcifications in 15 cases and as isolated microcalcifications in 2 cases.

The lesions were classified as "single" in 51 patients, while only one of them had more than one lesion.

Characteristics of study population are shown in Table 1.

Concerning the ICC analysis across different raters, the single-measure ICC for lesion volume was 0.986 (95% CI: 0.964-0.994; $p < 0.001$), indicating excellent reliability between the two raters.

3.2. Radiomic features analysis

The total number of extracted features was 195, classified in first order, second order and features from texture analysis. We extracted 18 intensity-based first-order statistical features, 24 Gray level cooccurrence matrix (GLCM) features, 16 Gray Level Size Zone Matrix (GLSZM) features, 5 neighborhood gray-tone difference matrix (NGTDM) features,

16 Gray Level Run Length Matrix (GLRLM) features, 14 Gray Level Dependence Matrix (GLDM) features and 9 2D shape features.

Correlation heat-maps showed that almost 3 radiomic features from tumor segmentations and 3 from gland segmentations were sufficiently independent to be used in the final model without redundancies. Hence, we set the number of selected features to 6 in the model including both tumor and gland features.

According to the AUC parameter, the best classifier for BRCA mutational status was Logistic Regression in all the models (Figures 8-10), followed by SVC in the model fitted with gland features and that fitted with both gland and tumor features and by Random Forest in the model fitted with tumor features only.

The model that showed better results was the one with gland features only (AUC = 0,827 for Logistic Regression as classifier) (Table 2-4).

The Delong's test showed a statistically significant difference ($p < 0,05$) between Logistic Regression and Decision Tree in the model with gland features only.

The features selected for the model fitted for the gland were Sum Entropy (GLCM), Size Zone Non-Uniformity Normalized (GLSZM) and 90thpercentile (first order).

The features selected for the comprehensive model were SumEntropy from gland (GLCM), RunEntropy from lesion (GLRLM), Gray Level Non-Uniformity from lesion (GLRLM), Minimum from lesion (first order), Small Area Low Gray Level Emphasis from lesion (GLSZM) and Median from gland (first order).

Eventually, selected features from tumor segmentation were Dependence Variance (GLDM), Energy (first order) and Kurtosis (first order).

GLCM Sum Entropy, a feature from texture analysis, which is inherently related to the qualitative characterization of the tissue [27] and to the randomness in the image values [28], was significantly higher in BRCA mutated patients in the model fitted with gland features only and in the comprehensive model (figure 11-12).

3.3. Association of non-radiomic features variables with the outcome

Among clinical characteristics, no statistically significant differences were observed between the two groups, probably due to the limited sample size. However, the BRCA mutated patients were sensibly younger than the BRCA non mutated ones (p value = 0,08) as we observed in our previous radiomics study about MRI already published [4].

4.0 DISCUSSION

Considering the results obtained from breast MRI radiomic analysis on patients with triple negative breast cancer (TNBC) regarding the possibility of distinguishing BRCA mutated and non-mutated patients, we considered the possibility to perform the same analysis in parallel on mammographic examinations on the same patients' group [4].

We therefore tried to evaluate the feasibility of a radiomic analysis on mammographic examinations.

In fact, in literature there are not many works of radiomic analysis performed on mammographic examinations [29], [30] but most of the breast literature has developed on MRI radiomic analysis and more recently on contrast enhancement mammography (CEM) [17].

However, previous studies about computer extracted mammographic texture features demonstrated that the digital mammographic images contain computer extractable information not captured during routine radiologic interpretation which may permit an improved real-time risk stratification of breast cancer among women undergoing screening mammography [31], [32], [33].

Other authors have used radiomic analysis to develop an algorithm capable of recognizing suspicious lesions in mammographic examination and characterizing them, reducing diagnostic errors, false positives and negatives[30]. So, since the patients on whom we conducted radiomic analysis in MRI also underwent mammographic examination at the time of diagnosis, we decided to perform the radiomic analysis even on the mammographic images to evaluate the outcome in comparison with the results previously obtained. As reported in the literature [5], the TNBC mammographic lesion most frequently presented was the mass with (15 cases) or without (36 cases) microcalcifications and this made

the lesion segmentation in the mammographic images easier. Manual segmentation performed on mammographic images allowed for the extraction of radiomic features from both tumor lesions and normal glandular tissue. We used a manual segmentation technique unlike other authors [30], considering the need to perform a different data extraction both from lesions defined as TNBC but also from areas of normal glandular tissue. Manual segmentation seemed to us the best technique also considering the different typology of lesions and the low number of cases.

We first considered separately the features from the tumor and the contralateral gland, then we performed another analysis with all the features together building three different models: a model with gland features only, a model with tumor features only and a comprehensive model with both tumor and gland features.

Correlation heat-maps showed that, among the 195 features initially extracted, almost 3 from tumor segmentations and 3 from gland segmentations were sufficiently independent to be used in the final model without redundancies. Hence, we set the number of selected features to 6 in the model including both tumor and gland features.

According to the AUC parameter, the best classifier for BRCA mutational status, among the four trained, was Logistic Regression in all the models, followed by SVC in the model fitted with gland features and in the one fitted with both gland and tumor features and by Random Forest in the model fitted with tumor features only. The model that showed better results was the one with gland features only (AUC = 0,827 for Logistic Regression), with accuracy of 77%, sensitivity of 80% and specificity of 93%.

In light of the results obtained we believe that healthy glandular tissue may represents a structurally more

homogeneous environment unlike tumor lesions in which, following neo-angiogenesis and cellular proliferation index, we can find necrosis and hemorrhage, sources of structural heterogeneity. Therefore, we believe genetic patterns can be more easily traced in glandular tissue. Similarly, combining the gland and tumor model, for the reasons outlined above, may reduce their predictive performance.

The results in terms of AUC related to the classifiers tested for the mutational status are superimposable to those obtained in the MR radiomic model. In particular, the linear logistic regression classifier shows the best results in both mammographic and MR radiomic models in association with the nonlinear SVC model. The same logistic regression model is confirmed to be reliable in other literature works that develop predictive mutation models integrated with clinical data [34], [35].

Considering the results of the literature, we evaluated the role of texture features extracted from glandular tissue in discriminating between BRCA-mutated and non-mutated patients to investigate the possibility of including radiomics in multifactorial risk assessment systems.

GLCM Sum Entropy, a feature from texture analysis which is related to the randomness in the image values [28], was significantly higher in BRCA mutated patients in the model fitted with gland features only and in comprehensive model.

Therefore, even our analysis has underlined the role of texture analysis features [27], [30]; previously, the work of S.G. Sapate et al. emphasized that considering the intrinsic limitations of mammographic examination, geometric features alone are unable to distinguish between benign and malignant lesions but that it is necessary to include texture analysis features such as gray level co-occurrence matrix (GLCM), in order to make the model reliable. The authors

include 48 textural and seven geometric features underlining the role of texture analysis in mammography radiomic analysis. The differences we found in texture radiomic feature GLCM Sum Entropy, according to BRCA mutation status, both in the model fitted with gland features only and in the comprehensive model may probably reflect underlying biological status: germline BRCA mutations are known to influence genomic stability, [36] and cellular differentiation, [37] potentially leading to biological alterations in breast tissue microarchitecture that could be captured by radiomic texture features such as GLCM Sum Entropy, which is related to the randomness in the image values [28]. In this context radiomic may detect gene-based biological patterns not visually appreciable on conventional imaging.

In agreement with our study, several works in literature have highlighted the importance of GLCM Sum Entropy and in general of texture analysis in oncology. [28], [38], [39], [40], [41]

This result indeed is in line with other works in the literature that emphasize the role of breast tumors texture analysis with radiomic extraction in the differentiation of TNBC and non-TNBC tumors and in the identification of androgen receptor-positive TNBC [40]; or the importance of similar texture analysis features in predicting malignancy of suspicious microcalcifications on CEM [28].

Similarly, in other works in the literature that consider PET CT, radiomic texture analysis is used with a predictive prognostic role in patients with lymph node metastases from an unknown primary tumor, or as predictor of Lynch syndrome and PDL-1 expression [38], [39].

Looking at the classification of breast density in the two populations, mutated and non-mutated, although we can see how in patients carrying the BRCA mutation, class B

absolutely prevails and in non-mutated patients there is a balanced subdivision between the B and C density patterns, as already reported in the literature, there are no significant differences in the BRCA mutated and non-mutated populations in the glandular density patterns and/or in the morphological characteristics of the tumor lesions in this case with triple negative molecular subtype [42].

On the other hand, as also highlighted in our previous work of MR radiomic analysis [4] and in other works in the literature [31], [32], [33], evidence emerges that the normal glandular tissue may contain information that do not result in a different glandular pattern at mammographic images and cannot be highlighted during the normal process of visualization and analysis by the radiologist but that can be detected by radiomic analysis and can distinguish patients based on their mutational status.

These results also strengthened the concept that mutational status can be associated with biological and molecular differences in glandular tissue that generate texture features able to discriminate between mutated and non-mutated populations.

In both radiomic analysis of TNBC in MRI and mammography, no features significantly associated with the mutational status emerged from the tumoral lesions. This suggests that, at a molecular level, TNBC probably has characteristics common to mutated and non-mutated patients.

Also, among clinical characteristics, no statistically significant differences were observed among the two groups, even if the BRCA mutated patients were sensibly younger than the BRCA non mutated ones (p value = 0,08) as we observed in our previous radiomics study already published.

As already highlighted in the literature, great interest has emerged in recent years to develop a mammography-based

deep learning tools for breast cancer prediction also in dataset from a high-risk population based on the detection of precancerous variations on the mammographic examination [26] or in investigating the association between phenotypic and genotypic characteristics of diseases, especially oncological ones, as an objective of the emerging chapter of precision medicine [20]. Our work fits into this chapter by looking for, through the radiomic analysis of biomedical big data contained in images, the relationships between genomic structure and TNBC, going further in the research for relationships between genomic structure and risk of developing breast cancer.

We explored the possibility of using texture radiomic analysis of glandular tissue in mammographic examination to predict genetic mutation risk and we obtained results that, if confirmed in large series of patients, suggest the possible development of AI tools based on radiological images to be inserted into risk assessment systems. [4][17]

Most of the literature on radiomics in breast cancer relies on MRI studies[17], as it is a multiparametric technique that allows for analysis of different data subsets (contrast enhancement, DWI, T2), offering a greater number of possibilities than mammography. However, mammography is a more widely available and used technique in the screening setting, therefore evaluating the feasibility and accuracy of radiomic analysis in mammography aims to identify a tool that can be incorporated into risk assessment systems applicable to large number of women.

This study has some limitations: First, due to its retrospective nature, mammographic examinations were not performed using the same mammograph, however, all examinations were acquired using digital mammography with standardized projections. Second, the sample size was limited;

nevertheless, the study population was highly selected and homogeneous, a feature that, while reducing variability, may also represent a source of bias. Eventually, the study lacks external validation, which could be achieved through future single-center or multi-center studies addressing the same research question.

5.0 CONCLUSIONS

This study demonstrates the feasibility of radiomic analysis applied to mammographic examinations and suggests a potential role for radiomic texture features of normal breast glandular tissue, analyzed using linear regression models, in discriminating BRCA mutation status.

These findings support the hypothesis that normal glandular tissue, rather than tumor tissue, may contain radiomic information reflecting underlying gene-driven biological and molecular differences. Overall, the results indicate that mammography could potentially be used not only as a screening tool but also as a non-invasive approach for patient stratification according to their mutational status and disease risk. However, it is important to underline that these findings should be considered preliminary and require confirmation in larger, independent, prospective multicenter studies and in radiomic models integrated with clinical data.

Data availability statement

The datasets analysed during the current study are available from corresponding author on reasonable request.

REFERENCES

- [1] Guarneri, V. *et al.* Preoperative carboplatin-paclitaxel- bevacizumab in triple-negative breast cancer: final results of the phase II Ca.Pa.Be

study. **Ann. Surg. Oncol.** 22(9), 2881–2887 (2015). 10.1245/s10434-015-4371-0

[2] Jiang, L. *et al.* Radiogenomic analysis reveals tumor heterogeneity of triple-negative breast cancer. **Cell Rep. Med.**3(7), 100694 (2022). 10.1016/j.xcrm.2022.100694

[3] Yin, L., Duan, J. J., Bian, X. W. & Yu, S. C. Triple-negative breast cancer molecular subtyping and treatment progress. **Breast Cancer Res.** 22, 61 (2020). 10.1186/s13058-020-01296-5

[4] Pecchi, A. *et al.* DCE-MRI radiomic analysis in triple-negative ductal invasive breast cancer: comparison between BRCA and non-BRCA mutated patients. **Magn. Reson. Imaging** 113, 110214 (2024). 10.1016/j.mri.2024.110214

[5] Karbasian, N. *et al.* Imaging features of triple-negative breast cancer and the effect of BRCA mutations. **Curr. Probl. Diagn. Radiol.** 50(3), 316–322 (2021). 10.1067/j.cpradiol.2020.01.011

[6] Ha, S. M. *et al.* Association of BRCA mutation types, imaging features, and pathologic findings in patients with breast cancer with BRCA1 and BRCA2 mutations. **AJR Am. J. Roentgenol.** 209(4), 920–928 (2017). 10.2214/AJR.16.16957

[7] Gareth, D. G. *et al.* Penetrance estimates for BRCA1 and BRCA2 based on genetic testing in a clinical cancer genetics service setting. **BMC Cancer** 8, 155 (2008). 10.1186/1471-2407-8-155

[8] Krammer, J. *et al.* Breast cancer detection and tumor characteristics in BRCA1 and BRCA2 mutation carriers. **Breast Cancer Res. Treat.** 163(3), 565–571 (2017). 10.1007/s10549-017-4198-4

[9] Incorvaia, L. *et al.* BRCA1/2 pathogenic variants in triple-negative versus luminal-like breast cancers: genotype–phenotype correlation in a cohort of 531 patients. **Ther. Adv. Med. Oncol.** 12, 1758835920975326 (2020). 10.1177/1758835920975326

[10] You, C. *et al.* Clinicopathological and MRI features of patients with BRCA1/2 mutations in familial breast cancer. **Gland Surg.** 10(1), 262–272 (2021). 10.21037/gs-20-596

[11] Gallivanone, F., Bertoli, G. & Porro, D. Radiogenomics, breast cancer diagnosis and characterization: current status and future directions. **Methods Protoc.** 5(5), 78 (2022). 10.3390/mps5050078

[12] Cè, M. *et al.* Artificial intelligence in breast cancer imaging: risk stratification, lesion detection and classification, treatment planning and prognosis. **Explor. Target Antitumor Ther.** 3, 113–127 (2022). 10.37349/etat.2022.00113

[13] Litvin, A. A. *et al.* Radiomics and digital image texture analysis in oncology. **Sovremennye Tehnologii v Medicine**13(2), 11 (2021). 10.17691/stm2021.13.2.11

[14] Siviengphanom, S. *et al.* Mammography-based radiomics in breast cancer: a scoping review of current knowledge and future needs. **Acad. Radiol.** 29(8), 1170–1182 (2022). 10.1016/j.acra.2021.09.025

- [15] Li, W. *et al.* Radiomics analysis combining gray-scale ultrasound and mammography for differentiating breast adenosis from invasive ductal carcinoma. **Front. Oncol.** 14, 1390342 (2024). 10.3389/fonc.2024.1390342
- [16] Lv, T. *et al.* AI-powered interpretable imaging phenotypes noninvasively characterize tumor microenvironment associated with diverse molecular signatures and survival in breast cancer. **Comput. Methods Programs Biomed.** 243, 107857 (2024). 10.1016/j.cmpb.2023.107857
- [17] Valdora, F. *et al.* Rapid review: radiomics and breast cancer. **Breast Cancer Res. Treat.** 169, 217-229 (2018). 10.1007/s10549-018-4675-4
- [18] Satake, H. *et al.* Radiomics in breast MRI: current progress toward clinical application in the era of artificial intelligence. **Radiol. Med.** 127, 141-150 (2022). 10.1007/s11547-021-01423-y
- [19] Mazurowski, M. A. Radiogenomics: what it is and why it is important. **J. Am. Coll. Radiol.** 12(8), 862-866 (2015). 10.1016/j.jacr.2015.04.019
- [20] Yin, X. X. *et al.* MRI radiogenomics for intelligent diagnosis of breast tumors and accurate prediction of neoadjuvant chemotherapy response — a review. **Comput. Methods Programs Biomed.** 212, 106510 (2022). 10.1016/j.cmpb.2021.106510
- [21] Mireştean, C. C. *et al.* Radiomics in triple-negative breast cancer: new horizons in an aggressive subtype of the disease. **J. Clin. Med.** 11(3), 616 (2022). 10.3390/jcm11030616
- [22] Qi, Y. J. *et al.* Radiomics in breast cancer: current advances and future directions. **Cell Rep. Med.** 5, 101719 (2024). 10.1016/j.xcrm.2024.101719
- [23] Kocak, B. *et al.* CLEAR checklist for evaluation of radiomics research. **Insights Imaging** 14, 215 (2023). 10.1186/s13244-023-01415-8
- [24] Balleyguier, C. *et al.* BI-RADS classification in mammography. **Eur. J. Radiol.** 61(2), 192-194 (2007). 10.1016/j.ejrad.2006.08.033
- [25] Deng, Y. *et al.* Radiomics models based on multi-sequence MRI for preoperative evaluation of MUC4 status in pancreatic ductal adenocarcinoma: a preliminary study. **Quant. Imaging Med. Surg.** 12(11), 5129-5139 (2022). 10.21037/qims-22-112
- [26] Omoleye, O. J. *et al.* External evaluation of a mammography-based deep learning model for predicting breast cancer in an ethnically diverse population. **Radiol. Artif. Intell.** 5(6), e220299 (2023). 10.1148/ryai.220299
- [27] Mavroforakis, M. E. *et al.* Mammographic masses characterization based on localized texture and dataset fractal analysis using linear, neural and support vector machine classifiers. **Artif. Intell. Med.** 37(2), 145-162 (2006). 10.1016/j.artmed.2006.03.002
- [28] Cao, K. *et al.* Peri-lesion regions in differentiating suspicious breast calcification-only lesions specifically on contrast enhanced

mammography. **J. Xray Sci. Technol.** 32(3), 583-596 (2024). 10.3233/XST-230332

[29] Ponsiglione, A. M. *et al.* A statistical approach to assess the robustness of radiomics features in the discrimination of mammographic lesions. **J. Pers. Med.** 13(7), 1104 (2023). 10.3390/jpm13071104

[30] Sapate, S. G. *et al.* Radiomics-based detection and characterization of suspicious lesions on full-field digital mammograms. **Comput. Methods Programs Biomed.** 163, 1-20 (2018). 10.1016/j.cmpb.2018.05.017

[31] Huo, Z. *et al.* Computerized analysis of digitized mammograms of BRCA1 and BRCA2 gene mutation carriers. **Radiology** 225(2), 519-526 (2002). 10.1148/radiol.2252010845

[32] Li, H. *et al.* Computerized analysis of mammographic parenchymal patterns for assessing breast cancer risk: effect of ROI size and location. **Med. Phys.** 31(3), 549-555 (2004). 10.1118/1.1644514

[33] Gierach, G. L. *et al.* Relationships between computer-extracted mammographic texture pattern features and BRCA1/2 mutation status: a cross-sectional study. **Breast Cancer Res.** 16(4), 424 (2014). 10.1186/s13058-014-0424-8

[34] Guo, R. *et al.* A nomogram model combining ultrasound-based radiomics features and clinicopathological factors to identify germline BRCA1/2 mutation in invasive breast cancer patients. **Heliyon** 10(1), e23383 (2024). 10.1016/j.heliyon.2023.e23383

[35] Deng, T. *et al.* Development and validation of ultrasound-based radiomics model to predict germline BRCA mutations in patients with breast cancer. **Cancer Imaging** 24, 76 (2024). 10.1186/s40644-024-00676-w

[36] Roy, R., Chun, J. & Powell, S. N. BRCA1 and BRCA2: different roles in a common pathway of genome protection. **Nat. Rev. Cancer** 12(1), 68-78 (2012). 10.1038/nrc3181

[37] Semmler, L., Reiter-Brennan, C. & Klein, A. BRCA1 and breast cancer: underlying mechanisms of tissue-specific tumorigenesis in mutation carriers. **J. Breast Cancer** 22(1), 1-14 (2019). 10.4048/jbc.2019.22.e6

[38] Ishiwata, Y. *et al.* Feasibility of prognosis assessment for cancer of unknown primary origin using texture analysis of 18F-FDG PET/CT images of largest metastatic lymph node. **Nucl. Med. Commun.** 42(1), 86-92 (2021). 10.1097/MNM.0000000000001310

[39] Wang, X. *et al.* Additional value of PET/CT-based radiomics to metabolic parameters in diagnosing Lynch syndrome and predicting PD-1 expression in endometrial carcinoma. **Front. Oncol.** 11, 595430 (2021). 10.3389/fonc.2021.595430

[40] Xu, W. J. *et al.* Identification of triple-negative breast cancer and androgen receptor expression based on histogram and texture analysis of dynamic contrast-enhanced MRI. **BMC Med. Imaging** 23, 102 (2023). 10.1186/s12880-023-01022-5

[41] Zhang, T., Li, X. & Liu, J. Prediction of the invasiveness of ground-glass nodules in lung adenocarcinoma by radiomics analysis using high-resolution computed tomography imaging. **Cancer Control** 29, 10732748221089408 (2022). 10.1177/10732748221089408

[42] Dontchos, B. N. *et al.* Are qualitative assessments of background parenchymal enhancement, amount of fibroglandular tissue on MR images, and mammographic density associated with breast cancer risk? **Radiology** 276(2), 371–380 (2015). 10.1148/radiol.2015142304
CRediT authorship contribution statement

Annarita Pecchi: Writing- original draft, Investigation, Data curation, Conceptualization.

Giulia Sessa: Writing-review & editing, Investigation, Data curation.

Luca Nocetti: Writing- review & editing, Software, Methodology, Formal analysis.

Cecilia Beretta: Writing - review & editing, Investigation, Data curation.

Chiara Bozzola: Writing- review & editing, Investigation. Erica Balboni: Writing - review & editing, Software, Methodology, Investigation.

Giulia Besutti: Writing- original draft, Methodology, Data curation, Conceptualization.

Angela Toss: Writing-review & editing, Investigation, Conceptualization.

Laura Cortesi: Writing - review & editing, Investigation, Conceptualization.

Gabriele Guidi: Writing- review & editing, Supervision, Investigation.

Massimo Dominici: Writing- review & editing, Supervision, Investigation.

Pietro Torricelli: Writing- review & editing, Supervision, Investigation.

Funding details

This study was partially supported by funding from the European Union-NextGenerationEU through the Italian Ministry of University and Research under PNRR -M4C2-I1.3 Project PE_00000019“HEAL ITALIA” to Giulia Besutti, E93C22001860006.

Ethical statement

The study has been approved by the local ethical committee.

Declaration of competing interest

The authors declare that they have no known competing financial interests or personal relationships that could have appeared to influence the work reported in this paper

TABLES

	BRCA- mutated (n = 13)	Non- BRCA- mutated (n = 39)	Overall (n = 52)
Characteristic			
Breast density			
A	2 (15.4%)	5 (12.8%)	7 (13.5%)
B	7 (53.8%)	13 (33.3%)	20 (38.5%)
C	2 (15.4%)	15 (38.5%)	17 (32.7%)
D	2 (15.4%)	6 (15.4%)	8 (15.4%)
Number of lesions	13	40	53
Lesion type			
Mass (nodule)	9 (69.2%)	27 (67.5%)	36 (67.9%)
Mass + microcalcifications	4 (30.8%)	11 (27.5%)	15 (28.3%)
Isolated microcalcifications	0 (0%)	2 (5.0%)	2 (3.8%)
Extent of disease			
Single lesion	13 (100%)	38 (97.4%)	51 (98.1%)
Multiple lesions	0 (0%)	1 (2.6%)	1 (1.9%)
Age (years)	44.9 ± 10.4	49.0 ± 8.9	48.0 ± 9.4

Data are presented as number (%) unless otherwise indicated. Breast density categories according to BI-RADS. Age is reported as mean ± standard deviation.

Table 1: Clinicopathological and mammographic characteristics of the study population according to BRCA mutation status

Model	AUC Mean (SD)	Accuracy Mean (SD)	Sensitivity Mean (SD)	Specificity Mean (SD)
SVC	0,79 (0,2)	0,75 (0,04)	0,6 (0,39)	0,9 (0,09)
Random Forest	0,75 (0,17)	0,73 (0,1)	0,8 (0,27)	0,83 (0,17)
Decision Tree	0,69 (0,18)	0,74 (0,13)	0,57 (0,25)	0,82 (0,13)
Logistic Regression	0,83 (0,16)	0,77 (0,04)	0,8 (0,16)	0,93 (0,1)

Table 2: Scores of the considered classifiers from the model fitted with gland features selected with MRMR.

Model	AUC Mean (SD)	Accuracy Mean (SD)	Sensitivity Mean (SD)	Specificity Mean (SD)
SVC	0,73 (0,16)	0,74 (0,06)	0,77 (0,2)	0,6 (0,27)

Random Forest	0,59 (0,23)	0,74 (0,09)	0,73 (0,25)	0,68 (0,22)
Decision Tree	0,61 (0,2)	0,66 (0,09)	0,53 (0,4)	0,75 (0,22)
Logistic Regression	0,73 (0,2)	0,72 (0,12)	0,87 (0,27)	0,83 (0,17)

Table 3: Scores of the considered classifiers from the model fitted with tumor features, selected with MRMR.

Model	AUC Mean (SD)	Accuracy Mean (SD)	Sensitivity Mean (SD)	Specificity Mean (SD)
SVC	0,41 (0,15)	0,76 (0,04)	0,8 (0,27)	0,65 (0,12)
Random Forest	0,6 (0,12)	0,7 (0,03)	0,8 (0,16)	0,65 (0,15)
Decision Tree	0,55 (0,09)	0,68 (0,07)	0,37 (0,22)	0,75 (0,14)
Logistic Regression	0,73 (0,13)	0,74 (0,07)	0,87 (0,16)	0,73 (0,12)

Table 4: Scores of the considered classifiers from the model fitted with both tumor and gland features, selected with MRMR.

RCC
FOR PRES
04/08/2020, 13:56:42
Esame: oggetto SR CAD non disponibile

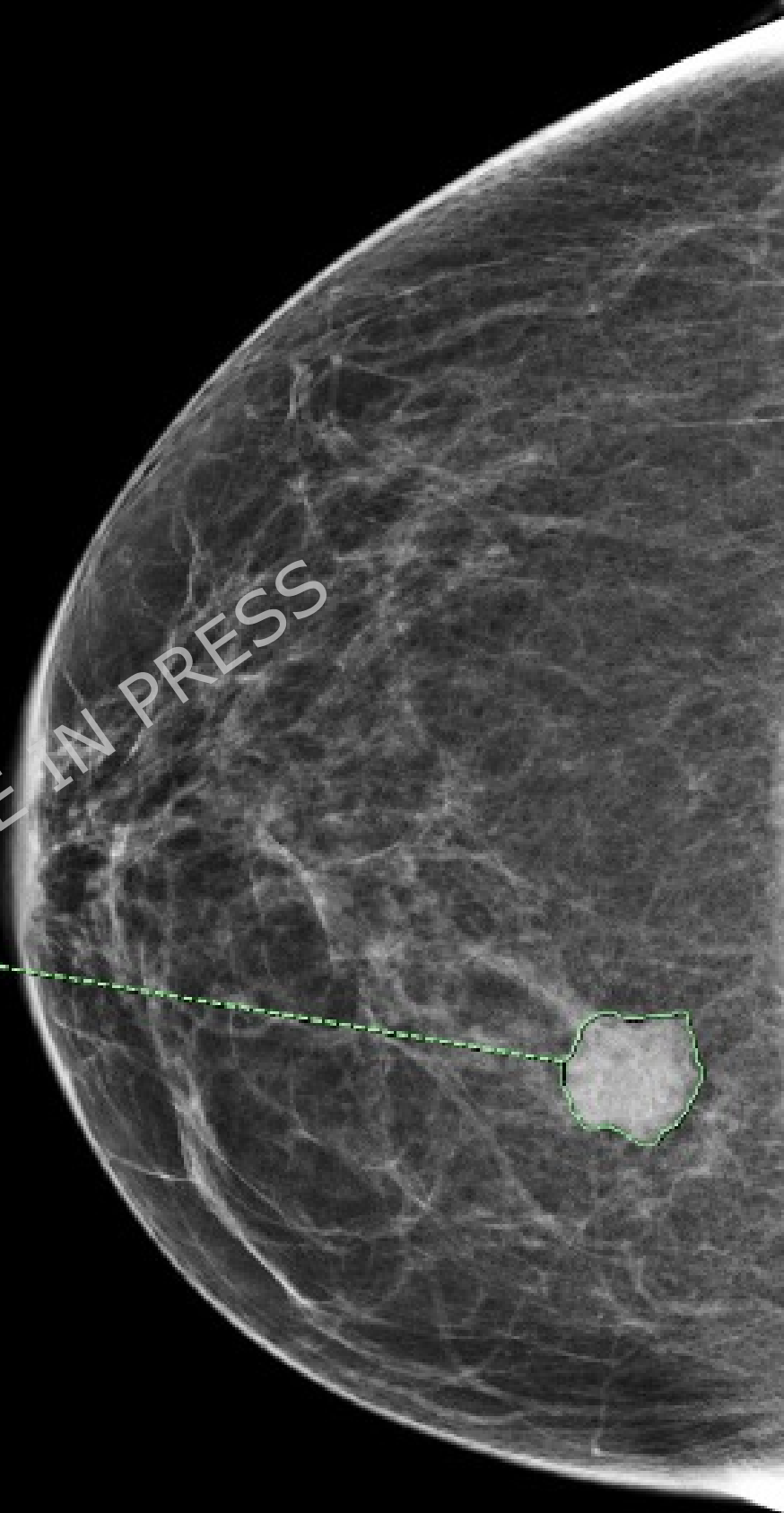
Density: ---

ARTICLE IN PRESS

A: 199,47 mm²
P: 57,53 mm
SD: 460 US
M: 2.576 US
Len Min: 15,94 mm
Lun magg.: 18,09 mm
Min: 658 US
Max: 3.568 US

FOV: ---mm
S: 245
Z: 0,308
C: 2047
W: 4096

TECNICO, TECNICO
SeleniaValuePlus
YM800804



RML
FOR PRES
27/05/2019, 11:00:37
Esame: oggetto SR CAD non disponibile

Density: ---

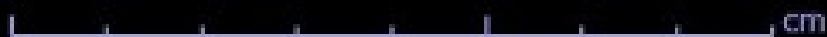
ARTICLE IN PRESS

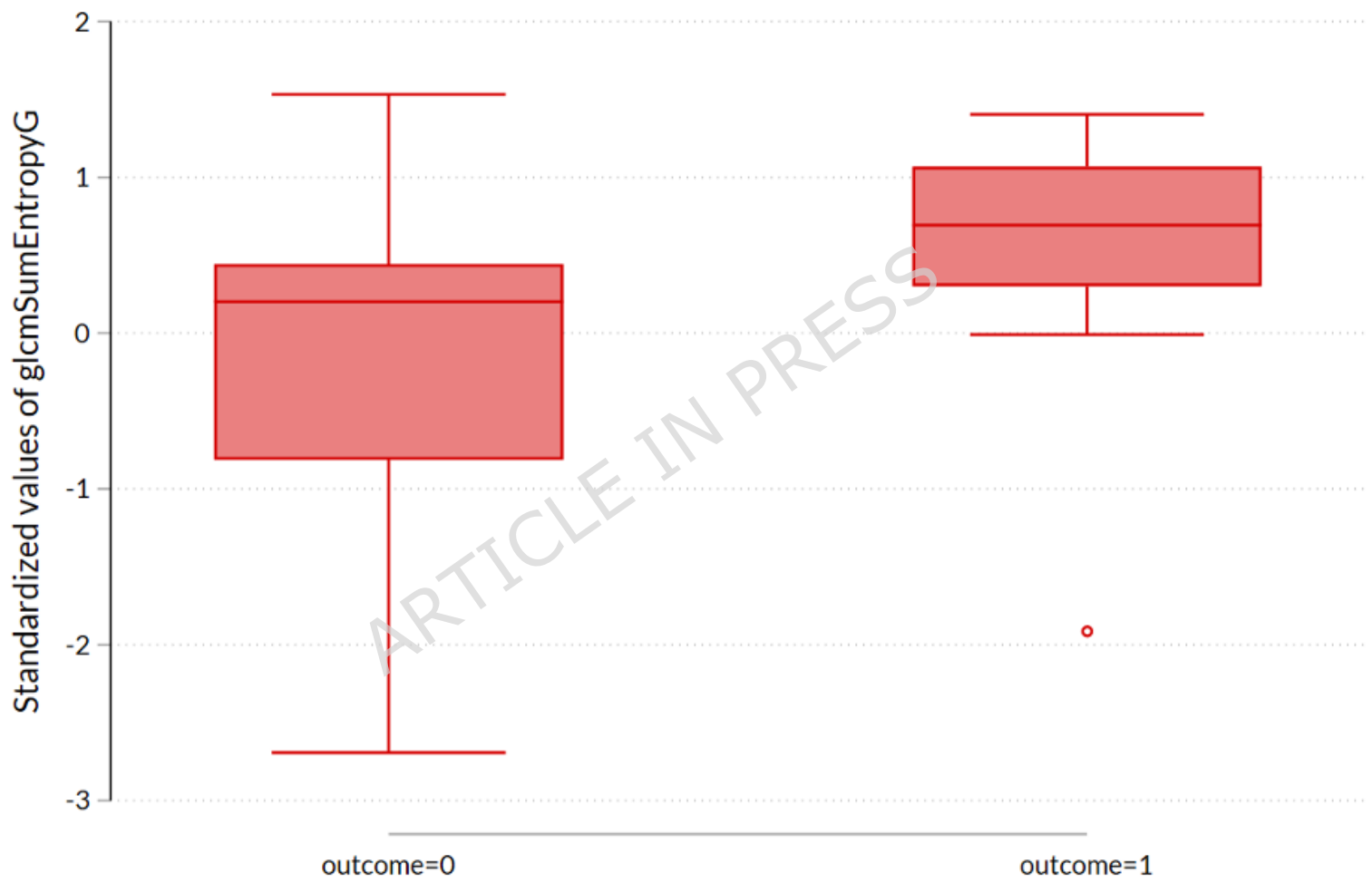
L: 58,21 mm

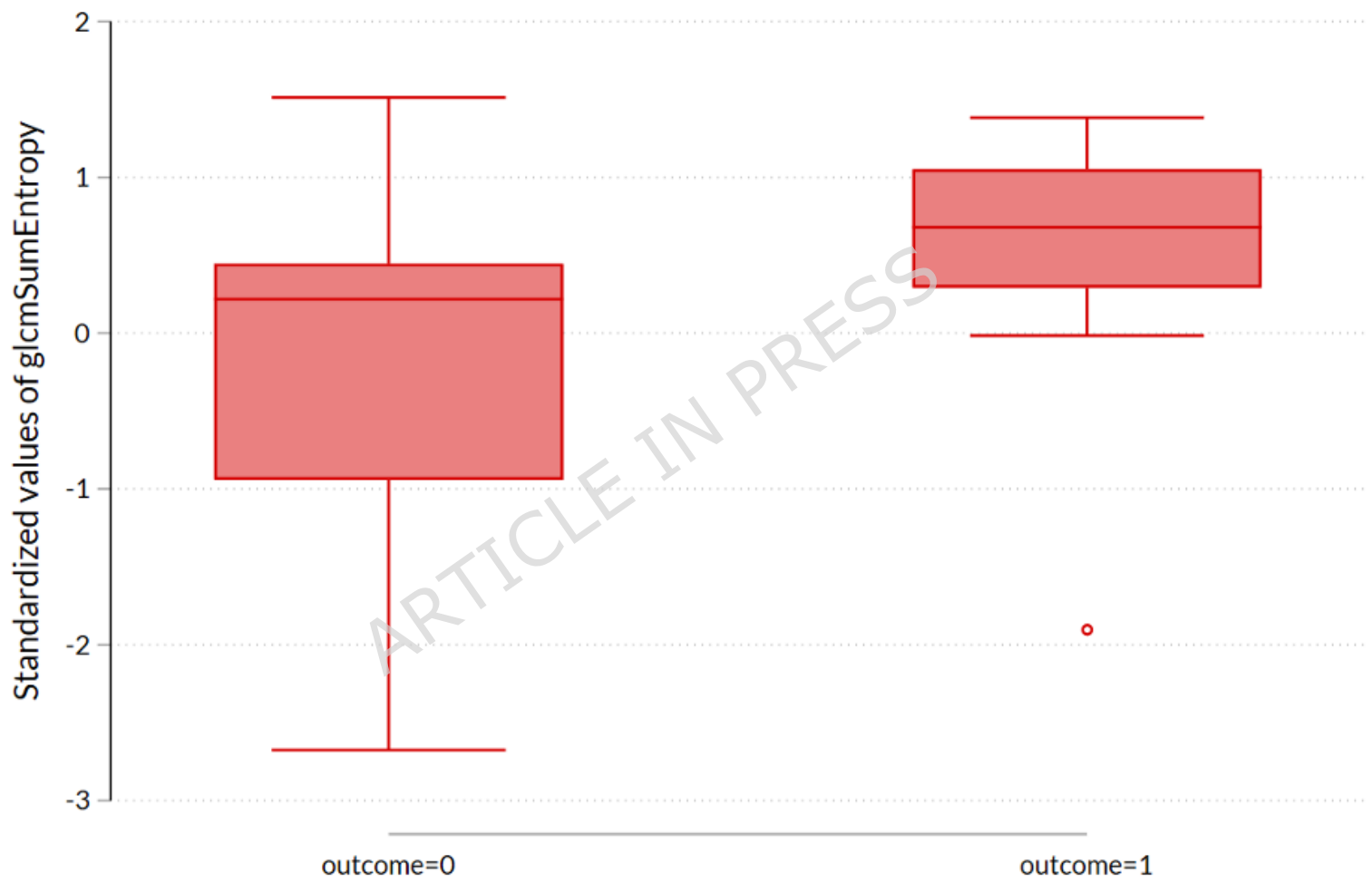


FOV: ---mm
S: 343
Z: 0,308
C: 2700
W: 3600

operatore
MghSCI
YM638353







IM: 26 SE: 71100000

LCC

LCC

FOR PRES

04/08/2020, 13:57:33

Esame: oggetto SR CAD non disponibile

Density: ---

A: 100,43 mm

P: 36,02 mm

SD: 355 US

M: 1.384 US

Len Min: 9,88 mm

Lun magg.: 12,95 mm

Min: 92 US

Max: 2.959 US



ARTICLE IN PRESS

FOV: ---mm

S: 244

Z: 0,308

C: 2047

W: 4096

TECNICO, TECNICO

SeleniaValuePlus

YM800804

LML
FOR PRES
11/06/2019, 11:06:01
Esame: oggetto SR CAD non disponibile

Density: ---

ARTICLE IN PRESS

A: 102,07 mm²
P: 35,99 mm
SD: 199 US
M: 2.596 US
Len Min: 10,51 mm
Lun magg.: 12,36 mm
Min: 1.805 US
Max: 3.332 US

FOV: ---mm
S: 341
Z: 0,308
C: 2700
W: 3600

operatore
MghSC1
YM638353

cm

Gland

